한국소음진동공학회 창립10주년 기념 소음진동학술대회논문집, pp. 1577~1582.

헤드 슬라이더의 실험적 모드해석

0전정일* 이용석** 박영필***

Experimental Modal analysis of Roll and Pitch of Head Slider

Jeong-Il Chun, Yong-Seok Lee and Young-Phil Park

ABSTRACT

In this study, the experimental modal analysis is performed to investigate the dynamic characteristics of slider-air bearings in hard disk drives. Bump response of the slider is acquired by measuring the relative velocity for two points using the laser interferometer, in which the disk is scratched lightly by a sharp knife to make a bump. From the measurements, the modal parameters of the head slider, modal frequencies and damping ratios of roll and pitch, are estimated by data processing and parameter estimation.

1. Introduction

Since the introduction of the first product, IBM RAMAC, in 1957, there has been a steady increase in recording density of hard disk drives. The first product has the areal recording density of 5Mbyte in the 24 inch fifty disks with the linear recording density of 100 bit/inch (BPI) and track recording density of 20 track/inch (TPI). But one of the recent products has 356 KBPI, 28.5 KTPI and 10.1 Gbits/sq.in^2 recording density. In this case, the improvement of recording density is the 3560 times in linear recording density, 1425 times in track and five million times in areal recording density. The increase of the linear recording density is primarily obtained by the reduction in the gap between magnetic field in the head, flying height between head and media, and the thickness of the recording layer in the media disk. In particular, to increase the recording density, the decrease of flying height is demanded. However, the possibility of the impact between slider and disk has been increased by the lowered flying height. Furthermore, the recent simulation results were reported that the change of thermal flow between slider and disk is affected by the slider's flying height, and can cause MR signal to be disarranged even though there is no contact. Consequently, it is important to control the change of flying height for the slider with MR head. The transient fluctuation of the slider is directly related to the dynamic characteristics of the slider-air bearing. The knowledge of head-disk interface is very important to make

* Dep. of Mech. Engineering, Yonsei Univ.
** Dep. of Mech. Engineering, Yonsei Univ.
*** Professor, Dep. of Mech. Engineering, Yonsei Univ.

the reliable head interface and to improve the performance of hard disk drive. Therefore, the evaluation of the dynamic properties of air-bearings, such as stiffness and damping ratio, becomes an important concern.

Many researchers have performed the simulation and experimental study on the dynamic characteristics of slider air bearing. C. A. Briggs and F. E. Talke measured the roll and pitch motion of slider and investigated the change of frequency according to the rotating speed of disk[1,2,3]. Q.H. Zeng and D.B. Bogy developed the slider-air bearing simulator and performed the modal analysis for the roll and pitch motion of slider[4,5,6,7]. They measured the roll and pitch motion of slider using LDV, and estimated modal frequencies and damping ratios.

In this paper, we estimated the modal frequencies and damping ratios of the roll and pitch motion of slider by measuring the bump response of slider.

2. Theoretical Background

2.1 Governing Equation

In this study, it is assumed that the slider is rigid body and the vibration of slider occurs near the steady flying height. With these assumptions, the state of slider behavior can be modeled as linear, time-invariant system. Furthermore, for the simplicity in the modal analysis, it is assumed that slider model is self-adjoint system and has viscous damping property. By the assumptions, the governing equation of the slider motion is expressed as

$$[M]\{\ddot{u}\}+[C]\{\dot{u}\}+[K]\{u\}=\{f(t)\} \quad (1)$$

where $[M]$,$[K]$ and $[C]$ are the mass, stiffness and damping matrices(3×3), respectively. $\{u\}=\{z,\theta,\beta\}^T$ is the displacement vector of the slider, in which z, θ and β are the vertical, pitch and roll displacement at the slider's mass center, respectively. The external force, $\{f(t)\}$, is assumed to be impact force, because exciting force is not applied after the slider passes the bump. From this assumption, the slider has three modes of vibration, and the dynamic behavior can be expressed as in equation (2) in frequency domain.

$$G(\omega)=\sum_{r=1}^{3}\left\{\frac{U_r+jV_r}{j(\omega-\omega_{dr})+\sigma_r}+\frac{U_r-jV_r}{j(\omega+\omega_{dr})+\sigma_r}\right\} \quad (2)$$

The equation (2) is expressed as

$$G(s)=\sum_{r=1}^{3}\left\{\frac{A_r}{(s-s_r)}+\frac{A_r^*}{(s-s_r^*)}\right\} \quad (3)$$

Performing the inverse Laplace transformation of Eq. (3) yields

$$h(t)=\sum_{r=1}^{3}\left(A_r e^{s_r t}+A_r^* e^{s_r^* t}\right) \quad (4)$$

$$s_r=-2\pi f_r\zeta_r+i2\pi f_r\sqrt{1-\zeta_r^2} \quad r=1,2,3 \quad (5)$$

where A_r is the modal participation factor (a complex constant), and ζ_r, f_r are the damping ratio and frequency of mode r, respectively.

2.2 Preprocessing

Because the signal-to-noise(S/N) ratio is poor in the experimental situations, the measured bump response can not be used directly to estimate the modal parameters. Therefore, it is necessary to perform data preprocessing to improve S/N ratio before the data is used in the parameter estimation.

1) Data truncation. To extract modal properties, only the free vibration responses after the slider has passed over bumps are required. Therefore, we used the response data after the second peak, which is shown in Fig.1.

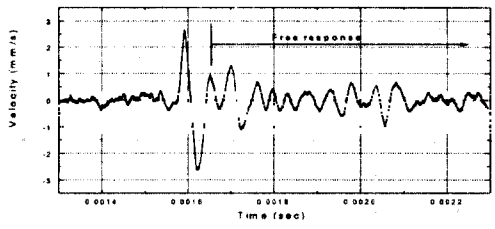

Fig. 1 Bump response of trailing edge center

2)Band pass filtering. Our main interest is only the vibration of slider-air bearing. Therefore, we filtered the data using a digital band pass filter with a pass band of 20 kHz to 200 kHz.

3)Filtering in the time domain. The response measured with any noises and disturbances can be expressed as

$$h_m(t) = h(t) + n(t) \tag{6}$$

where $h(t)$ is the true free response of slider according to the bump excitation and $n(t)$ is the random noise, in which the response of the random disturbances and the measurement noise are included. Assuming that the response of the slider is not correlated with noise, the auto-correlation function of $h_m(t)$ can be expressed as

$$\begin{aligned} R_{h_m h_m}(\tau) &= \int_0^\infty \left(\sum_{r=1}^{2N} A_r e^{s_r(t+\tau)} \sum_{k=1}^{2N} A_k e^{s_k t} \right) dt + R_{nn}(\tau) \\ &= \sum_{r=1}^{2N} \left\{ A_r e^{s_r \tau} \int_0^\infty \left(\sum_{k=1}^{2N} A_k e^{(s_k + s_r)t} \right) dt \right\} + R_{nn}(\tau) \end{aligned} \tag{7}$$

or

$$R_{h_m h_m}(\tau) = \sum_{r=1}^{2N} (B_r e^{s_r \tau}) + R_{nn}(\tau) \quad \tau \geq 0 \tag{8}$$

where $R_{nn}(\tau)$ is the auto-correlation function of $n(t)$, in which B_r has constant value. If $n(t)$ is the white noise, $R_{nn}(\tau)$ becomes dirac delta function, and the auto-correlation function of the measured response $h_m(t)$ can be written as

$$R_{h_m h_m}(t) = \sum_{r=1}^{2N} B_r e^{s_r t}. \quad t > 0 \tag{9}$$

Equation (9) is equivalent to Eq. (4). Therefore, we can calculate the auto-correlation of the measured response to eliminate the uncorrelated noises, and we can directly use these functions to estimate the modal frequencies and damping ratios.

4)Exponential window. The free response of the slider is rapidly damped out, and the S/N ratio is decreased. Consequently, we apply a weight function to the data that will be used in the parameter estimation. The exponential function is used, such as

$$W(t) = e^{-t/T_w} \quad t \geq 0, \tag{10}$$

where T_w is the coefficient of the window. After window is applied, the modal frequencies f_r and damping ratios ζ_r can be calculated by the estimated modal frequencies f' and damping ratios ζ', as follows

$$\begin{cases} \omega_r = \sqrt{\omega'^2 - 2\zeta'\omega'/T_w + 1/T_w^2} \\ \zeta_r = (\zeta'\omega' - 1/T_w)/\omega_r \end{cases} \tag{11}$$

2.3 Modal parameter Estimation

Equation (2) can be transformed to

$$\begin{aligned} G(\omega) &= \sum_{r=1}^{3} \left\{ \frac{U_r + jV_r}{j(\omega - \omega_{dr}) + \sigma_r} + \frac{U_r - jV_r}{j(\omega + \omega_{dr}) + \sigma_r} \right\} \\ &= \sum_{r=1}^{3} \left\{ \frac{2(\sigma_r U_r - \omega_{dr} V_r) + 2j\omega U_r}{[(\sigma_r^2 + \omega_{dr}^2) - \omega^2] + 2j\sigma_r \omega} \right\}. \end{aligned} \tag{12}$$

Introducing $s = j\omega$,

$$\begin{aligned} G(s) &= \sum_{r=1}^{3} \left\{ \frac{p_r s + q_r}{s^2 + 2\zeta_r \omega_r s + \omega_r^2} \right\} \\ &= \sum_{r=1}^{3} \frac{N_r(s)}{D_r(s)}. \end{aligned} \tag{13}$$

If we know the r^{th} mode responses from the numerical or experimental analysis, the error function can be constructed as

$$\varepsilon(s) = h_r(s)\, D_r(s) - N_r(s). \tag{14}$$

Using the least square method, the coefficient $N_r(s)$ and $D_r(s)$ can be obtained, so that the norm of the errors in a specified frequency band is minimized.

3. Experimental setup and procedure

The schematic diagram of experimental setup is shown in Fig. 2. The experimental setup includes a spin-stand, a two-beam Laser Doppler Vibrometer, an oscilloscope, and a computer. The disk equipped on the spin stand motor is scratched lightly by a sharp knife to make a bump. The disk is rotated to 5400rpm, the slider is located at 19.5mm from the center of disk in the radial direction and the relative velocity between disk and slider is 11m/s.

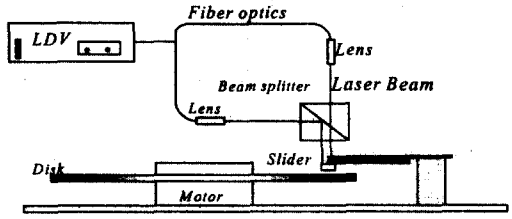

Fig. 2 Schematic of measurement method

The Polytec OFA512 LDV is used to measure the velocity response of slider according to the bump excitation. Before the measurement of the slider dynamics, the profile of a bump is measured at the measuring position on the disk to acquire the good impulse excitation. The relative velocity of the two points on the slider is measured by the two laser beams of the LDV. The sliders used in measurement are the negative nano sliders(2.02×1.6×0.43mm) with sub-ambient pressure region.

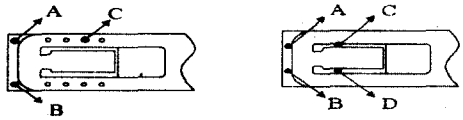

Type A HGA Type B HGA - cut

Fig. 4 Slider-gimbal assemblies and measurement points

Each HGA is attached on the same suspension and the outline of each gimbal is similar except that Type A HGA has the holes at gimbal. The point A and B are the trailing edge of the slider, which can be directly measured. In case of Fig. 4(a), fortunately the point C can be measured through the hole in the gimbal. However the point C and D in Fig 4(b) is difficult to measure because these are hidden by suspension. Therefore, the suspension is cut so that the point C and D can be measured. The time response of slider is observed and stored as data using the LeCroy LT344 oscilloscope, and then used to estimate the modal parameters after signal processing.

4. Experimental results

4.1 Type A HGA

Fig. 5 shows the roll response measured between point A and B of the Type A HGA. Fig. 5(a) shows the raw data measured by LDV during the slider pass through the bump.

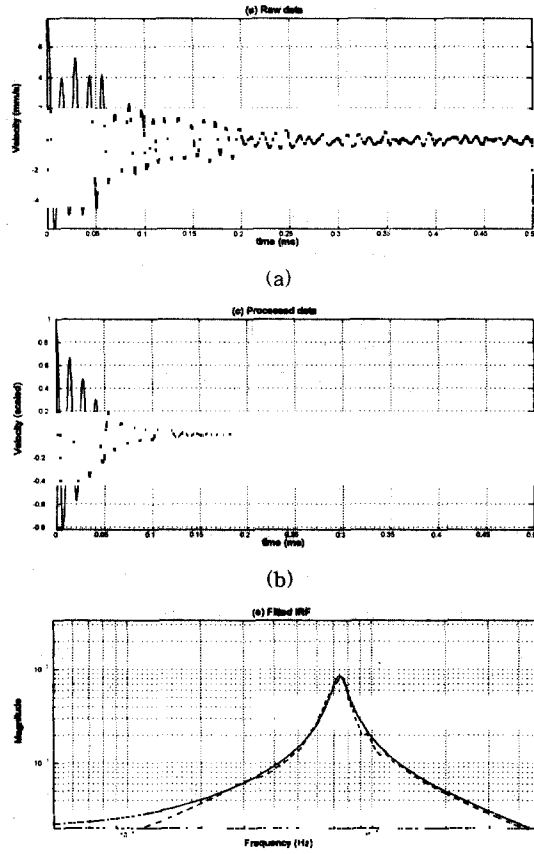

(a)

(b)

(c)

Fig. 5 Roll response between point A and B (Type A HGA)

The data in Fig. 5(a) is filtered to eliminate the influence of noise and disturbance, as shown in Fig. 5(b). Fig. 5(c) shows the impulse response function obtained using Fourier Transformation and curve fitting to estimate the

modal parameters. In this case, only the roll mode at the frequency of 73.4 kHz is obtained, which means that point A and B are on the nodal line of the pitch mode vibration. Fig. 6 shows the results measured to investigate the pitch motion of the system between the point A and C. In this case, three modes of vibration are observed, and the modal frequencies and damping ratios of all peaks are estimated using the curve fitting method. From the results in Fig 5, we can find that the mode around 70 kHz is roll mode of system. That means the nodal line of the roll mode is not parallel to the central line of the slider. According to the characteristics and simulation results for the general nano slider, other modes at 35.1 kHz and 114.6 kHz are estimated as the first and second pitch mode, respectively.

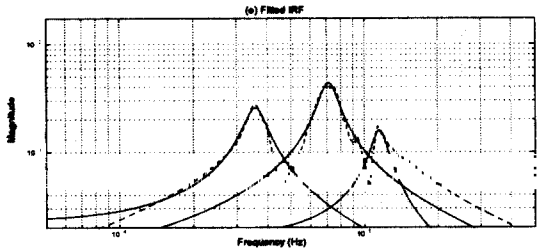

Fig. 6 Pitch response between point A and C (Type A HGA)

By the parameter estimation, the first pitch mode has the damping ratio of 5.8%, the roll mode has 4.7%, and the second pitch mode has 5.9%.

4.2 Type A slider - cut

Fig. 7 shows the roll response of Type A HGA mounted on the cut suspension. The frequency of the peak is estimated as 79kHz, which is 6kHz higher than the result before the suspension is cut in Fig 5. The damping ratio of roll mode vibration is estimated as 5.4 %.

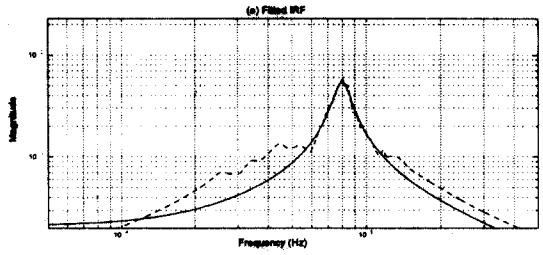

Fig. 7 Roll response between point A and B (Type A HGA - cut)

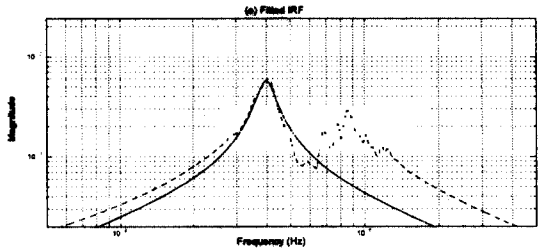

Fig. 8 Pitch response between point A and C (Type A HGA - cut)

The pitch mode is estimated that the natural frequency is 39.3 kHz and damping ratio is 4.3 %, which is shown in Fig. 8.

Comparing Fig 5 and Fig 7, it is found that the natural frequencies are increased and the damping ratios are decreased slightly. That is caused that the slider motion changes the surface contact from the point contact by the elimination of dimple point. Therefore, because the constraint of motion increases, the frequencies are shifted up.

4.3 Type B slider -cut

Fig. 9 and Fig. 10 are the response of the Type B HGA between point A and B, A and C, respectively. The frequencies of two peaks in Fig. 10 are estimated as 39.5 kHz and 73.1 kHz, respectively. From the results in Fig 9, we can interpret that the second peak, 73.1 kHz, is the roll mode of the system, and the peak around 40 kHz is pitch mode.

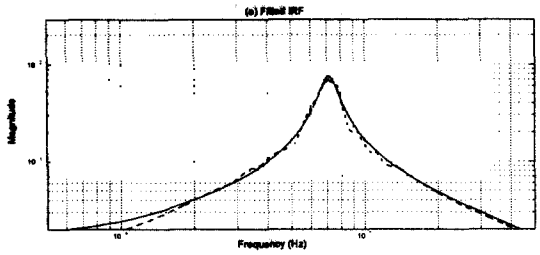

Fig. 9 Roll response between point A and B
(Type B HGA - cut)

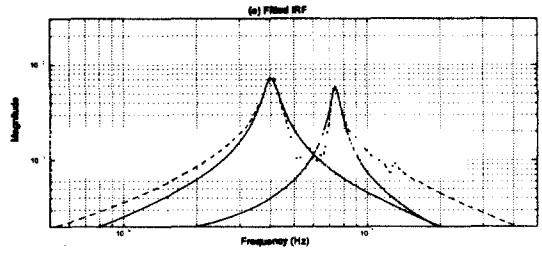

Fig. 10 Pitch response between point A and C
(Type B HGA - cut)

Comparing the results of Type A HGA with Type B, the frequencies of the pitch mode coincide around 40 kHz, but the roll modes have 10 kHz difference each other. The nodal line of pitch mode is parallel to the leading and trailing edge, and the roll mode is not parallel to the central line of the slider. For the damping ratio, the roll modes are almost similar, but, in the case of pitch modes, Type A HGA is very larger than Type B.

5. Conclusion

The dynamic characteristics of slider-air bearing in hard disk drive are experimentally studied. To investigate the dynamic properties of slider-air bearing, the time response of slider is measured using LDV. To excite the vibration of slider, slightly scratched disk is used to generate impulse like force. Some fitting techniques are applied to remove the effect of noise and disturbance, and the modal parameters of the system such as natural frequency and damping ratio are estimated from filtered signals. Two different nano sliders are used in the modal analysis, and the resulting characteristics are compared.

Reference

[1] C. A. Briggs, F. E. Talke, "An Investigation of the IBM 3380 K Slider Using Laser Doppler Interferometry", IEEE Transactions On Magnetics, Vol. 25, No. 5, September 1989, pp. 3707-3709.

[2] C. A. Briggs, F. E. Talke, "The Dynamics of Micro Sliders Using Laser Doppler Vibrometry", IEEE Transactions On Magnetics, Vol. 26, No. 5, September 1990, pp. 2442-2444.

[3] C. A. Briggs, F. E. Talke, "Investigation of the Dynamics of 50% Sliders Using Laser Doppler Vibrometry", IEEE Transactions On Magnetics, Vol. 26, No. 6, November 1990, pp. 3027-3032.

[4] Q. H. Zeng, D. B. Bogy, "Experimental Evaluation of Stiffness and Damping of Slider Air Bearings in Hard Disk Drives", Journal of Tribology, Vol. 121, January 1999, pp. 102-107.

[5] Q. H. Zeng, L. S. Chen, D. B. Bogy, "A Modal Analysis Method For Slider-Air Bearings In Hard Disk Drives", IEEE Transactions On Magnetics, Vol. 33, No. 5, September 1997.

[6] Q. H. Zeng, D. B. Bogy, " Stiffness and Damping Evaluation of Air Bearing Sliders By Modal Analysis Methods : New Designs With High Damping", Journal of Tribology.

[7] Q. H. Zeng, D. B. Bogy, "Dynamics of Suspension-Slider-Air Bearing Systems : Experimental Study", IEEE/ASME Transactions On Mechatronics, Vol. 3, No. 3, September 1998.